

Supplementary material to manuscript "High-resolution modelling of early contrail evolution from hydrogen-powered aircraft"

Annemarie Lottermoser and Simon Unterstrasser

Deutsches Zentrum für Luft- und Raumfahrt, Institut für Physik der Atmosphäre, Oberpfaffenhofen, Germany

Correspondence: Annemarie Lottermoser (annemarie.lottermoser@dlr.de)

1 Evaluation of z_{atm} and z_{emit}

In the ice crystal loss parametrization, the two length scales z_{atm} and z_{emit} are implicitly defined. In the original version in U2016 (= Unterstrasser, 2016), the non-linear equations were solved using a numerical method (classical bisection method). To speed up evaluations and to provide explicit formulations, fit formulae for the two length scales z_{atm} and z_{emit} were derived as outlined in Sec. (A3) of this study. In order to compare both versions simulation-wise, the length scale values determined with the bisection method and the fit formulae are compared. Moreover, the corresponding survival fractions based on either evaluation method are calculated. The outcomes are provided in Tab. S1. As already summarized in the main text of the present study: "Applying the analytical relations to calculate the parametrized survival fraction, we observe no change in 44 % of the data points (when rounded to two digits, as done in Tab. A1) and a maximum deviation of 2.0 %. A detailed comparison is provided in Tab. S1."

2 Comparison of the original and new ice crystal loss parametrization

The original ice crystal loss parametrization proposed in U2016 has been implemented in several larger-scale contrail models to refine the contrail initialization in those models (Gruber et al., 2018; Bier and Burkhardt, 2022), and applications were confined to conventional kerosene contrails.

This section presents comparison plots between the original and updated version of the ice crystal loss parametrization. Figure S1 shows scatter plots of z_{Δ} (panel (a)) and the parametrized survival fraction $\hat{f}_{N,s}$ (panel (b)), with the x -axis representing the original (2016) values and the y -axis showing the updated (2025) data. The values of z_{Δ} are similar across both formulations, although $z_{\Delta,2025}$ is generally slightly lower. However, differences in z_{Δ} should not be over-interpreted as this quantity serves as argument in an arctan-type function (see Eq. (12)) to retrieve the survival fraction. The arctan-type function formulation includes three fit coefficients that change from one to the other version. Hence, panel (b) shows the eventual differences in the parametrized survival fraction from the two versions. Likewise, $\hat{f}_{N,s}$ exhibits only minor scatter between the two versions.

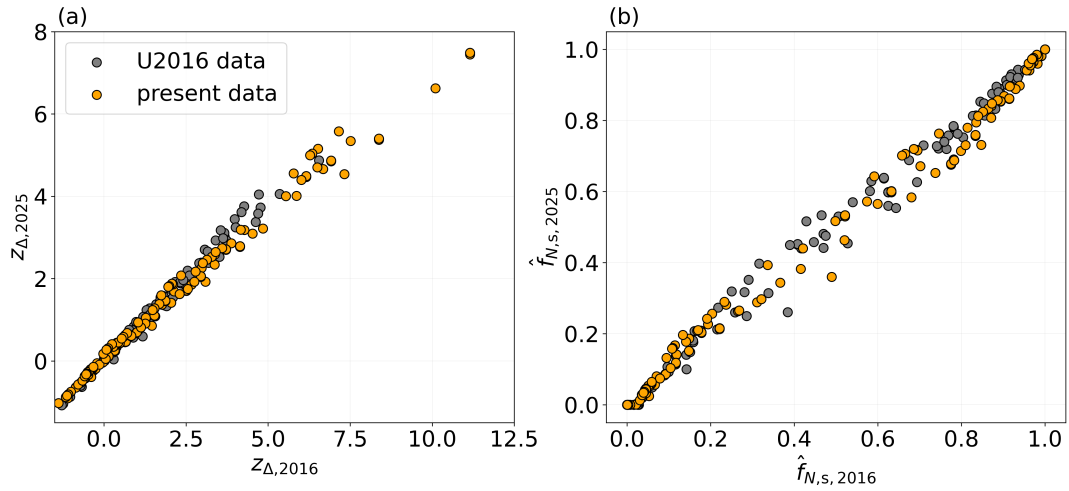


Figure S1. Scatter plot comparing the 2016 z_{Δ} values with the z_{Δ} values from the present study (a), and a similar comparison for the parametrized survival fractions (b).

Furthermore, we reproduce plots that were shown in U2016 (Figs. 5, 9, and 10 in that publication). In the new versions of those plots (Figs. S2-S4 in this document), we juxtapose the outcome of the original and the new parametrization. This should demonstrate that the switch to the new formulation has only marginal implications on applications focusing on conventional kerosene contrails.

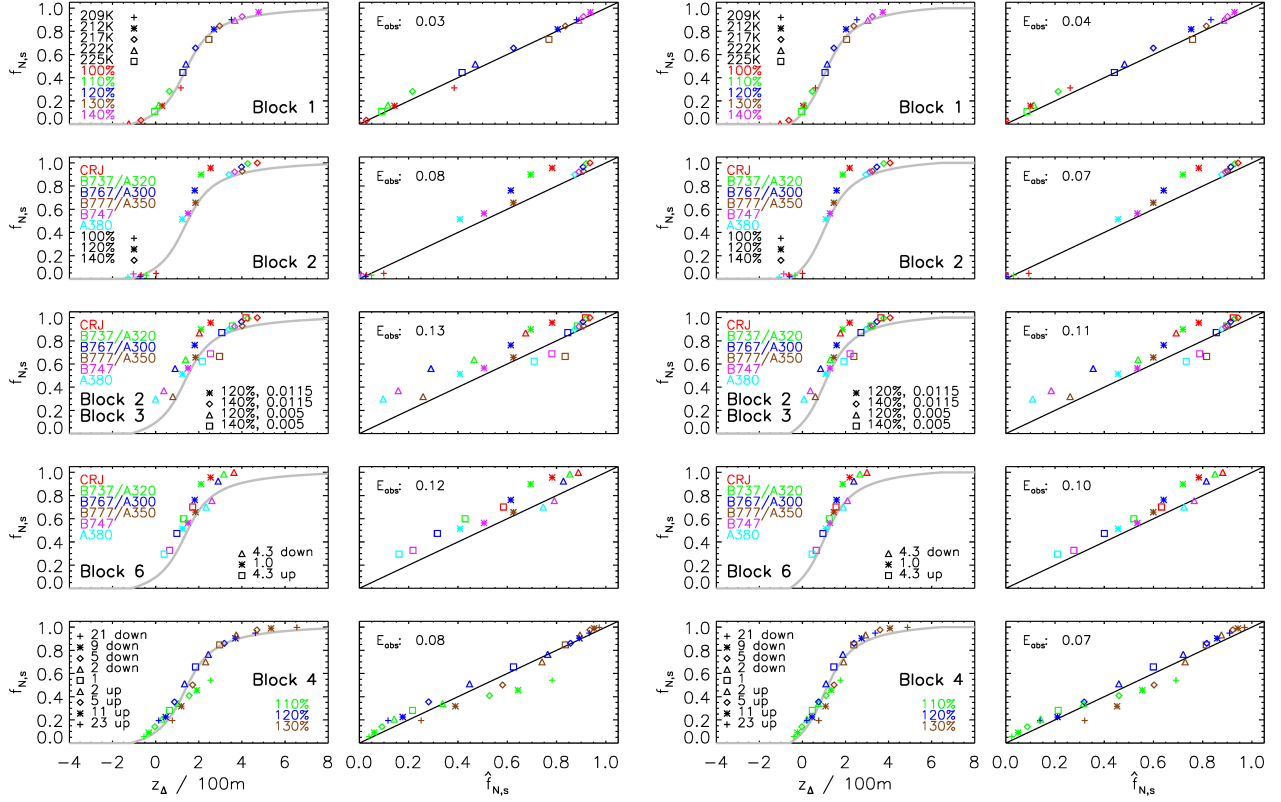


Figure S2. Reproduced version of Fig. 5 in U2016. The first two columns show the original plot from U2016. The third and fourth column use the parametrized survival fractions as obtained from the new parametrization version described in the present study.

Adapted figure caption of U2016:

Columns 1 and 3: Relationship between simulated survival fraction $f_{N,s}$ and z_{Δ} . The grey curve shows the fit function \hat{a} as defined in Eq. (12) in the present study.

Columns 2 and 4: Relationship between simulated survival fraction $f_{N,s}$ and approximated survival fraction $\hat{f}_{N,s}$. The black line shows the one-to-one line. Each row shows a subset of simulations taken from various simulation blocks defined in Table A2 of U2016. For example, the first row shows simulations of block 1, where RH_i and T_{CA} are varied. The legend in the plot provides a list of the symbols and colors, which uniquely define the simulations parameters of each plotted data point. The root mean square of the absolute error $\hat{f}_{N,s} - f_{N,s}$ is denoted as E_{abs} and given for each subset.

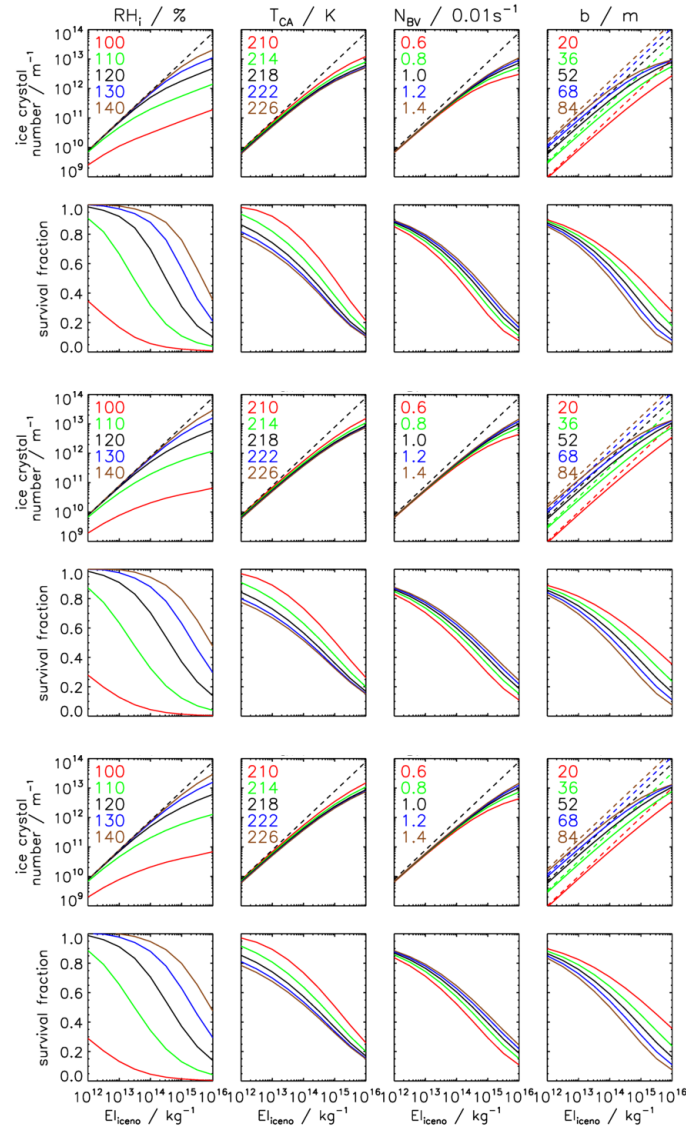


Figure S3. Reproduced version of Fig. 9 in U2016. The first two rows show the original plot from U2016. The other rows use the parametrized survival fractions as obtained from the new parametrization version described in the present study evaluating z_{atm} and z_{emit} either via bisection (rows 3&4) or by employing the fit functions (rows 5&6).

Adapted figure caption of U2016:

Sensitivity of ice crystal loss to El_{ice} for various values of RH_i , T , N_{BV} , and b (from left to right). See legend for the color coding. Rows 1, 3, and 5: Ice crystal number per meter of flight path before and after the vortex phase (dashed and solid curves). Note that the initial ice crystal number depends only on b and El_{ice} (following Eq. (A10) in U2016, which assumes a water vapor emission index of 1.25 kg/kg). Hence, only one dashed curve is shown in the columns for RH_i , T , and N_{BV} , respectively. Rows 2, 4, and 6: Survival fraction.

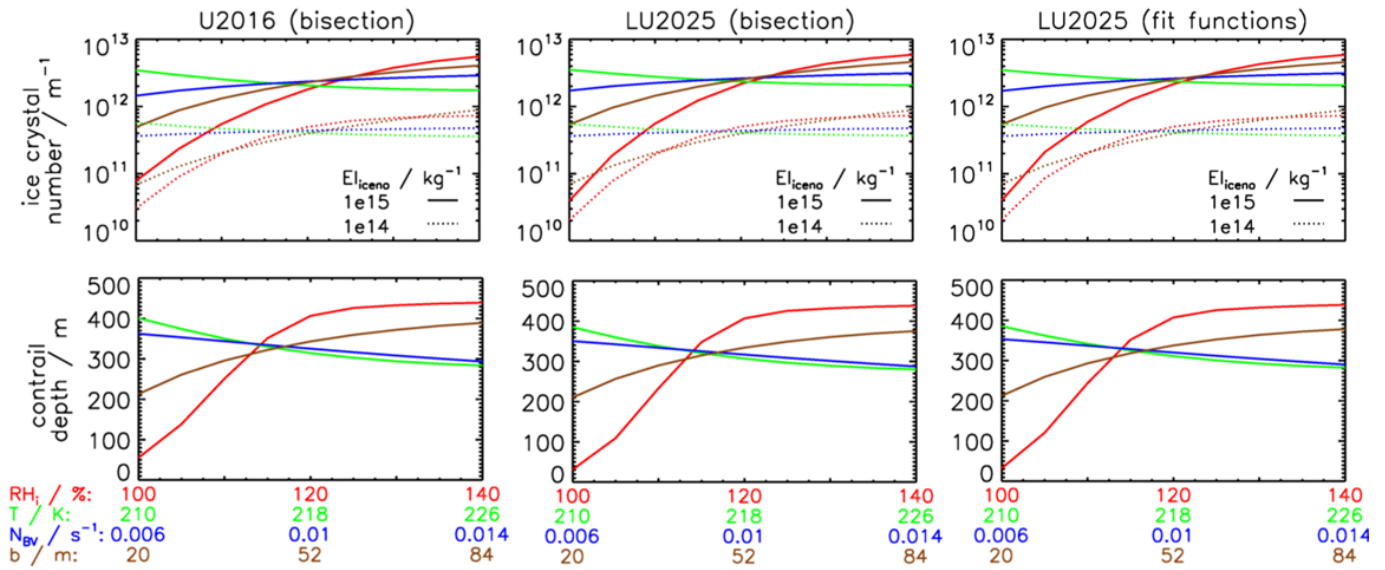


Figure S4. Reproduced version of Fig. 10 in U2016. The first column show the original plot from U2016. The two other columns use the new parametrization version (for both types of z_{atm} and z_{emit}).

Adapted figure caption of U2016:

Ice crystal number per meter of flight path (top) and contrail depth (bottom) after the vortex phase as a function of RH_i , T , N_{BV} , or b . EI_{ice} is 10^{15} or 10^{14} kg^{-1} . The contrail depth parametrization does not depend on EI_{ice} . Note that the parametrization of the contrail depth H was not updated in the present study. The slightly different results come from the fact that the parametrization of H uses the parametrized $f_{N,s}$ value as input. Note that the original plot in U2016 showed an additional panel with ice crystal number concentrations, which is left out here.

References

- Bier, A. and Burkhardt, U.: Impact of Parametrizing Microphysical Processes in the Jet and Vortex Phase on Contrail Cirrus Properties and Radiative Forcing, *J. Geophys. Res.*, 127, e2022JD036 677, <https://doi.org/10.1029/2022JD036677>, 2022.
- 30 Gruber, S., Unterstrasser, S., Bechtold, J., Vogel, H., Jung, M., Pak, H., and Vogel, B.: Contrails and their impact on shortwave radiation and photovoltaic power production – a regional model study, *Atmos. Chem. Phys.*, 18, 6393–6411, <https://doi.org/10.5194/acp-18-6393-2018>, 2018.
- Unterstrasser, S.: Properties of young contrails - a parametrisation based on large-eddy simulations, *Atmos. Chem. Phys.*, 16, 2059–2082, <https://doi.org/10.5194/acp-16-2059-2016>, 2016.

Nr	$\hat{f}_{N,s}$	$\tilde{f}_{N,s}$	z_{atm}	$\tilde{z}_{\text{atm}} / \text{m}$	$z_{\text{emit}} / \text{m}$	$\tilde{z}_{\text{emit}} / \text{m}$
1,2,3,4,5	0.06, 0.23, 0.6, 0.87, 0.97	0.05, 0.21, 0.59, 0.87, 0.98	164	163	249	250
6,7,8,9,10	0.0, 0.06, 0.22, 0.58, 0.86	0.0, 0.05, 0.22, 0.59, 0.87	85	87	249	250
11,12,13,14,15,16	0.05, 0.2, 0.57, 0.85, 0.96, 1.0	0.05, 0.19, 0.55, 0.86, 0.97, 1.0	164	163	546	541
17,18,19,20,21	0.08, 0.29, 0.68, 0.9, 0.98	0.08, 0.28, 0.68, 0.91, 0.99	85	87	546	541
22,23,24	0.06, 0.6, 0.97	0.05, 0.59, 0.98	164	163	249	250
25,26,27	0.06, 0.6, 0.97	0.05, 0.59, 0.98	164	163	249	250
28,29,30	0.0, 0.21, 0.86	0.0, 0.21, 0.87	85	87	249	250
31,32,33	0.0, 0.22, 0.86	0.0, 0.22, 0.87	85	87	249	250
34,35,36	0.2, 0.85, 1.0	0.19, 0.85, 1.0	164	163	546	541
37,38,39	0.2, 0.85, 1.0	0.19, 0.86, 1.0	164	163	546	541
40,41,42	0.08, 0.68, 0.98	0.08, 0.68, 0.99	85	87	546	541
43,44,45	0.08, 0.68, 0.98	0.08, 0.68, 0.99	85	87	546	541
46,47,48	0.0, 0.26, 0.94	0.0, 0.25, 0.95	164	163	249	250
49,50,51	0.0, 0.02, 0.73	0.0, 0.02, 0.74	85	87	249	250
52,53,54	0.02, 0.71, 1.0	0.01, 0.7, 1.0	164	163	546	541
55,56,57	0.0, 0.36, 0.96	0.0, 0.35, 0.97	85	87	546	541
Simulations at higher ambient temperatures						
58,59,60,61,62	0.03, 0.14, 0.44, 0.79, 0.94	0.02, 0.13, 0.43, 0.8, 0.95	177	176	110	112
63,64,65,66,67	0.0, 0.01, 0.09, 0.3, 0.69	0.0, 0.0, 0.09, 0.31, 0.7	92	95	110	112
68,69,70,71,72	0.08, 0.28, 0.67, 0.9, 0.98	0.07, 0.27, 0.67, 0.9, 0.99	177	176	262	263
73,74,75,76,77	0.0, 0.07, 0.27, 0.65, 0.89	0.0, 0.07, 0.27, 0.66, 0.9	92	95	262	263
78,79,80,81,82	0.05, 0.21, 0.57, 0.86, 0.97	0.05, 0.2, 0.56, 0.86, 0.97	186	185	163	163
83,84,85,86,87	0.0, 0.03, 0.15, 0.46, 0.81	0.0, 0.03, 0.15, 0.47, 0.82	97	99	163	163
88,89,90,91,92	0.05, 0.19, 0.53, 0.84, 0.96	0.04, 0.17, 0.52, 0.84, 0.96	191	191	123	121
93,94,95,96,97	0.0, 0.02, 0.12, 0.38, 0.76	0.0, 0.02, 0.12, 0.39, 0.77	99	102	123	121
98,99,100	0.04, 0.53, 0.96	0.04, 0.52, 0.96	191	191	123	121
101,102,103	0.05, 0.53, 0.96	0.04, 0.52, 0.97	191	191	123	121
104,105,106	0.0, 0.12, 0.76	0.0, 0.12, 0.77	99	102	123	121
107,108,109	0.0, 0.12, 0.76	0.0, 0.12, 0.77	99	102	123	121
110,111,112,113,114	0.04, 0.18, 0.52, 0.83, 0.96	0.04, 0.16, 0.5, 0.83, 0.96	195	194	102	99
115,116,117,118,119	0.0, 0.01, 0.1, 0.34, 0.73	0.0, 0.01, 0.1, 0.35, 0.74	101	104	102	99
Simulations with A320/B737-like aircraft						
120	0.72	0.72	164	163	176	183
121,122,123	0.13, 0.64, 0.96	0.12, 0.64, 0.97	177	176	76	79
124,125,126	0.03, 0.21, 0.78	0.03, 0.21, 0.8	92	95	76	79
127,128,129	0.2, 0.76, 0.99	0.19, 0.76, 0.99	177	176	185	186
130,131,132	0.07, 0.39, 0.9	0.06, 0.4, 0.91	92	95	185	186
133,134,135	0.17, 0.72, 0.98	0.16, 0.72, 0.98	186	185	114	113
136,137,138	0.04, 0.29, 0.85	0.04, 0.29, 0.86	186	185	114	113
139,140,141	0.16, 0.71, 0.97	0.15, 0.7, 0.98	191	191	85	83
142,143,144	0.04, 0.26, 0.82	0.03, 0.26, 0.83	99	102	85	83
145,146,147	0.16, 0.7, 0.97	0.15, 0.69, 0.98	195	194	70	67
148,149,150	0.03, 0.24, 0.81	0.03, 0.24, 0.82	101	104	70	67

Table S1. List of parametrized survival fractions derived with length scales that are computed via the numerical (Eqs. (6) and (7)) or the analytical method (Eqs. (A2) and (A3)), denoted with a tilde, and the corresponding length scales. Rows with three, five, or six simulations correspond to sets where the N_0 -scaling factors 100, 1, 0.01; 100, 10, 1, 0.1, 0.01; or 100, 100, 10, 1, 0.1, 0.01 are applied, respectively.